

General Disclaimer

One or more of the Following Statements may affect this Document

- This document has been reproduced from the best copy furnished by the organizational source. It is being released in the interest of making available as much information as possible.
- This document may contain data, which exceeds the sheet parameters. It was furnished in this condition by the organizational source and is the best copy available.
- This document may contain tone-on-tone or color graphs, charts and/or pictures, which have been reproduced in black and white.
- This document is paginated as submitted by the original source.
- Portions of this document are not fully legible due to the historical nature of some of the material. However, it is the best reproduction available from the original submission.

~~DECLASSIFIED~~

SPT

ETRS

NASA-CR-174049

E85-10026

(E85-10026 NASA-CR-174049)
SPECTRORADIOMETRIC CALIBRATION OF THE
THEMATIC MAPPER AND MULTISPECTRAL SCANNER
SYSTEM Quarterly Report, 1 May - 1 Aug.
1984 (Arizona Univ., Tucson.) 42 p

N85-11439

Unclass
G3/43 00026

SEVENTH QUARTERLY REPORT
ON

"SPECTRORADIOMETRIC CALIBRATION OF THE
THEMATIC MAPPER AND MULTISPECTRAL SCANNER SYSTEM"

Contract Number NAS5-27382
For the Period: 1 May 1984 - 1 August 1984

NASA/Goddard Space Flight Center
Greenbelt MD 20771

James M. Palmer, Co-Investigator
Philip N. Slater, Principal Investigator

Optical Sciences Center
University of Arizona
Tucson, Arizona 85721



INTRODUCTION

This is the seventh quarterly report on Contract NAS5-27382 entitled, "Spectroradiometric Calibration of the Thematic Mapper and the Multispectral Scanner System." In this report, we summarize the reduction of the data measured on July 8, 1984 at White Sands, New Mexico. The radiances incident at the entrance pupil of the Landsat 5 sensors have been computed for bands 1-4. When these are compared to the digital counts of the TM image, we will have the ground based calibration of this sensor. The image has been received from Goddard SFC and is presently being analyzed.

JULY 8, 1984 CALIBRATION

Field Measurements

This was our first opportunity to acquire on-site measurements at White Sands in conjunction with Thematic Mapper imagery from Landsat 5. Imagery was not available for previous trips due to cloud cover. Assisting in the field measurements were Harumi Aoki, Ken Castle, Barbara Capron, Madgeleine Dinguirard, Ron Holm, Ray Jackson, Carol Kastner, Amy Phillips, Rich Savage, and Phil Slater. The instrumentation on hand included two Barnes radiometers, the cart and yoke, an old model of Reagan's radiometer, both of the Castle spectropolarimeters, four polycorders, a printer, the Compaq computer, and two 2 X 2 ft standard reflectance panels.

Sunrise on the morning of July 8th was at 6:10 a.m. New Mexico was on Mountain Daylight Time (MDT) this time of year, as are the times quoted here. The Reagan instrument was set up and began acquiring solar irradiance measurements at 7:15 a.m. (airmass 4). Rich Savage took temperature, humidity, and pressure readings there at Chuck site. He also arranged for a nearby radiosonde ascent. These data are presented in Appendix B.

Two test sites had been laid out on the previous trip. Each was a 4 X 4 pixel grid, aligned with the east/west scan lines expected of Landsat. A road with a 120° bend separated the two sites, and will facilitate the identification of the sites on the digital TM imagery. Each site was measured with a Barnes radiometer. Starting at the center of

each 30 X 30 meter pixel, five reflectance measurements were taken of the gypsum sands, within an area of about 5. X 0.5 meters. Reflectance panel readings were taken periodically during the course of these measurements. (Both the BaSO₄ and Halon panels were recalibrated by Che Nianzeng immediately upon our return.) The data were averaged and recorded on polycorders. The site to the North of the road was scanned using the Purdue radiometer (one of the Barnes), mounted on the cart with the BaSO₄ panel. Data were taken from 11 to 11:20 a.m. The south site was scanned simultaneously with an USDA Barnes attached to a yoke. A Halon panel was used as the reference here. In addition to the two 4 X 4 pixel areas, two small areas were scanned near the van. This was done between 10:20 and 11:40 a.m. These areas were selected for their contrast, representing extremes of light and dark for the local area. They will later be used in conjunction with aerial photography to map the reflectance of the entire area. Finally, diffuse to direct measurements were taken between 8:30 and 10:20 a.m. These were made by comparing the radiance reflected from the ground to that radiance measured when the sun was blocked with a styrofoam parasol. These data can be used for comparison with the radiative transfer code, to verify our atmospheric models.

A helicopter overflight was arranged for this trip. Jack Rees and co-pilot Keys piloted the helicopter and Jason Penny, PFC, was the photographer. The flight was almost exactly one full hour. It had the dual purpose of recording radiance at intermediate altitudes, again for comparison to the radiative transfer code output, and photographing the sites. Several slides have been scanned, using a microdensitometer, and will be used to characterize the ground reflectance. Five rolls of

Ektachrome, ASA 100, were shot. All photos were taken at 1/500th of a second, with a 200 mm focal length lens. A series were taken at 6,000, 2,000, and 500 ft., AGL (above ground level). The photos were bracketed from F/16 to F/22, in half F/stop increments. Those taken at 2,000 ft. were particularly suited to our needs. Eight colored ground cloths had been laid out to define the two 4 X 4 pixel areas that were measured with the Barnes. We noted that the blue and orange ground cloths were the most visible from the air, as well as being the easiest to see on the color slides.

The field tests of the newly constructed spectropolarimeters will have to wait for our next trip to White Sands. The helicopter instrument suffered from a power failure, and data from the ground instrument, used for solar irradiance measurements, were lost during the TRS-80 to Compaq transfer. Back-up equipment was, however, available that enabled us to conduct an approximate calibration described in the following.

Langley Plot Computations

The Reagan radiometer was cycled through its narrowband filter set 95 times during the course of the morning. Each data set included, to the nearest second, a start and finish time and a voltage reading for each of the 9 spectral filters. These data were used as input to a program which computed solar zenith angle from ephemeris data. Using a refraction correction, airmasses were then calculated for each measurement. Finally, a weighted least squares analysis was used to compute the slope of the natural log voltages versus airmass, at each wavelength. The computed slopes are equivalent to the spectral optical depths of the atmosphere, τ_{ext} , at the time of overpass. Temporal

stability of the atmosphere is assumed. These results are given in Table 1. Also shown are the optical depth components τ_{Mie} , τ_{Ray} , and τ_{Oz} . The computation of these components is discussed next.

Using measured atmospheric pressure (883 mbar), τ_{Ray} can be easily computed. After subtracting this from τ_{ext} , a curve is plotted, as in Figure 1a, which contains only Mie and ozone components. To determine τ_{Mie} a curve is fit through all the $\tau_{ext} - \tau_{Ray}$ data points that do not include absorption. Normally this is done by submitting the optical depth values to a routine which fits the data to an equation of the form $\log \tau_{Mie} = a_0 + a_1 \log \lambda + a_2 (\log \lambda)^2$. As many of the spectral filter data sets were rejected, an alternate approach was taken here. These problems arose because the older of the two Reagan radiometers was used. On this instrument the heater was not functioning. The data are less reliable without the temperature stabilization, due to fluctuations in detector responsitivity. This problem is thought to have affected mainly the 0.872 and 1.03 μm channels.

Instead of our normal procedures, therefore, a manual fitting of the data was performed. A curve of the form $\log \tau_{Mie} = a_0 + a_1 \log \lambda$ was assumed (a straight line on this log-log plot). This is an approximation, valid only if the aerosols can be correctly modeled as obeying a Junge radial size distribution, $dn/dr = c r^{-(\nu+1)}$. In such a case the data would fall exactly on a line whose slope, a_1 , yields the Junge parameter ν via the relationship $a_1 = -\nu + 2$. By using only the 0.440 and 0.780 μm data points, a slope was determined. At these wavelengths the ozone absorption coefficients are small. Actually, the 0.440 and 0.872 μm pair is preferred, as the absorption coefficients are approximately equal. The

Table 1. Langley Plot Results.

Data from Reagan Radiometer
8 July, 1984
Chuck Site, White Sands, New Mexico

Latitude	32.935°
Longitude	106.407°
Right Ascension	7.226228 hours
Declination	22.365361°
Difference (Dec)	-419.3 arc-sec
Earth-Sun Distance	1.016701 AU
Pressure	883. mbar

WAV(μm)	τ _{ext}	τ _{Mie}	τ _{Ray}	τ _{oz}
0.4000	0.4426	0.0981	0.3172	0.0000
0.4400	0.3060	0.0922	0.2138	0.0006
0.5217	0.1921	0.0824	0.1063	0.0127
0.6120	0.1543	0.0743	0.0555	0.0246
0.6708	0.1091	0.0699	0.0382	0.0098
0.7120	0.1063	0.0673	0.0300	0.0046
0.7797	0.0842	0.0634	0.0208	0.0027
0.8717	0.0948	0.0589	0.0133	0.0006
1.0303	0.1103	0.0528	0.0068	0.0000

$$\log \tau_{Mie} = a_0 + a_1 \log \lambda; \quad \lambda \text{ in } \mu\text{m}$$

$$a_0 = -1.269 \quad a_1 = -0.654$$

$$\tau_{Ray} = \frac{29123.7 (n^2 - 1)^2}{\lambda^4}$$

$$n = 6432.8 + \frac{2949810}{146 - \lambda^2} + \frac{25540}{41 - \lambda^4}$$

λ in micrometers

$$\tau_{oz, \lambda} = NOZ * \alpha_{\lambda}$$

NOZ = columnar ozone

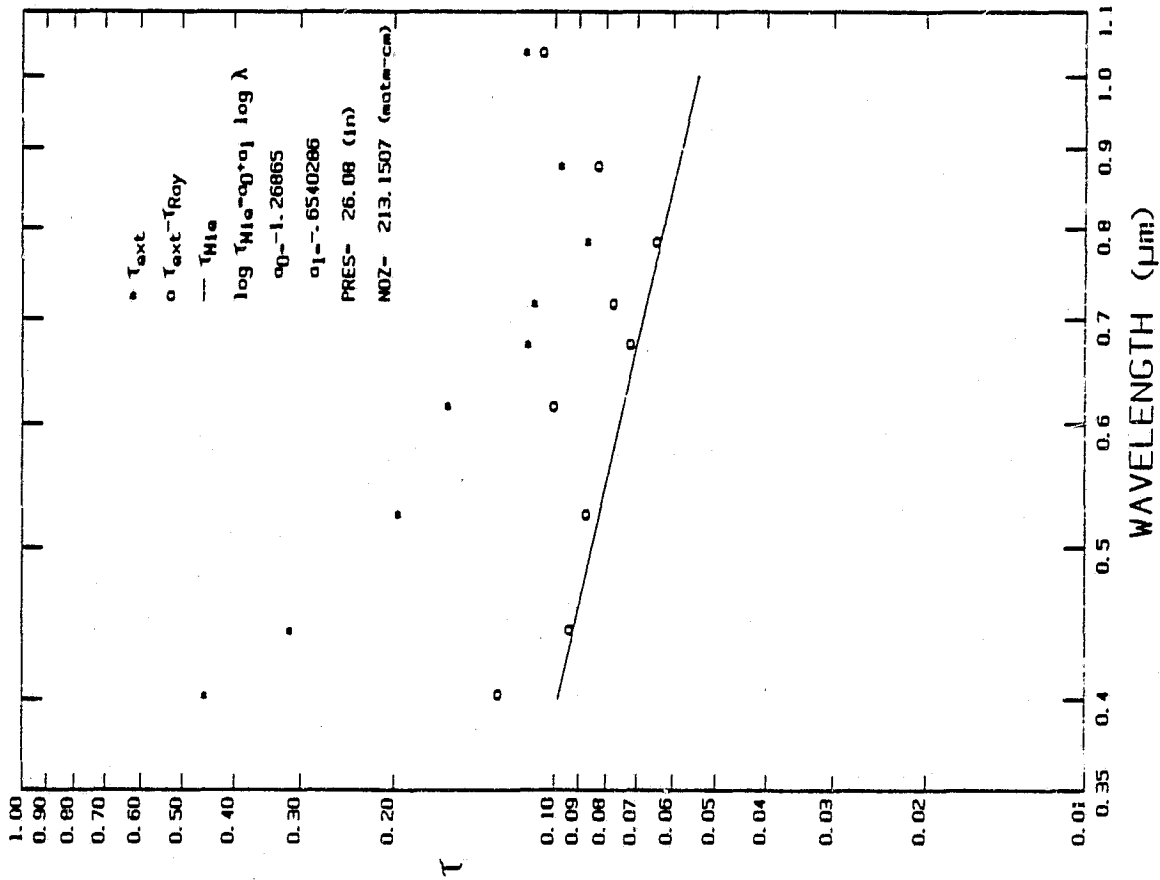
$$= \frac{\tau_{oz, 0.612 \mu\text{m}}}{\alpha_{0.612 \mu\text{m}}} = 213.2 \text{ matm-cm}$$

α = spectral absorption coefficient

Table 2. Spectral components for TM midband wavelengths.

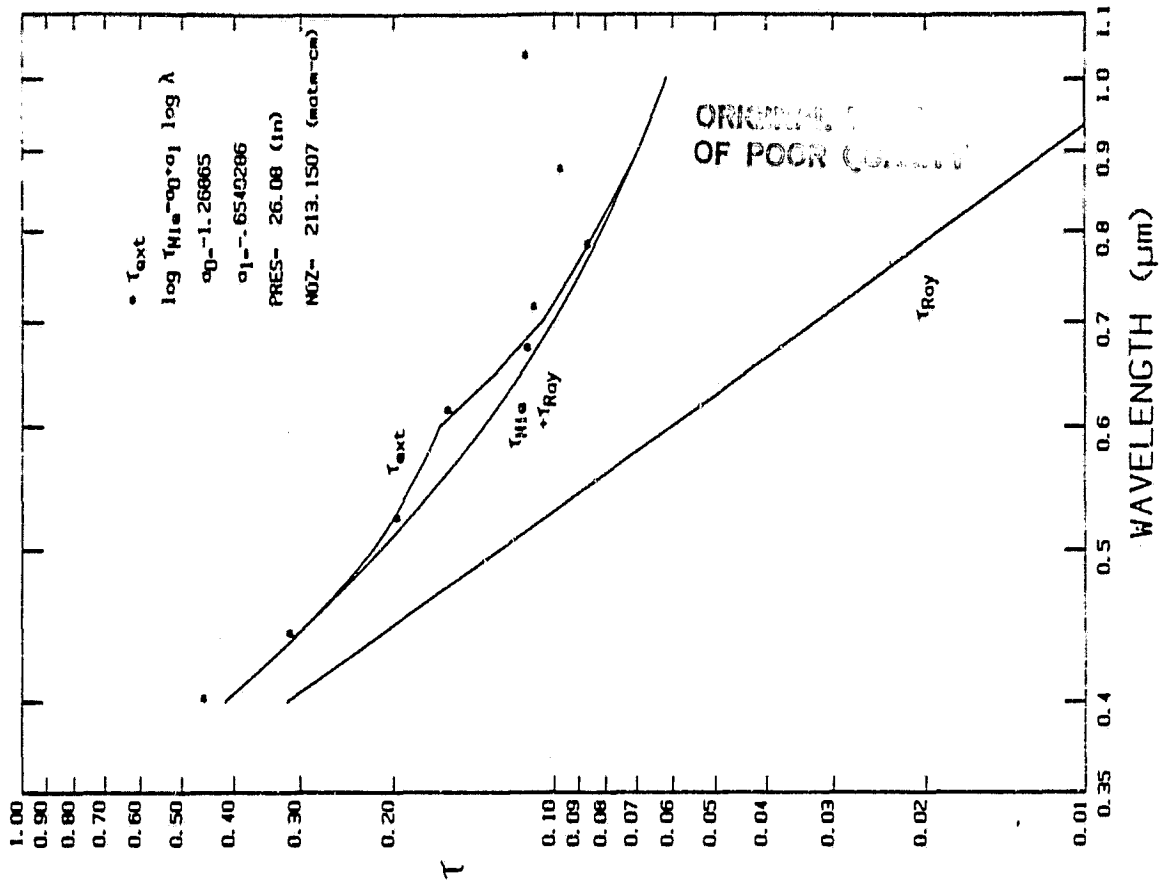
WAV (μm)	τ _{ext}	τ _{Mie}	τ _{Ray}	τ _{oz}	E ₀ (mW/cm ²)
0.486	0.2339	0.0864	0.1421	0.0055	175.955
0.571	0.1745	0.0777	0.0735	0.0232	180.580
0.661	0.1226	0.0706	0.0406	0.0114	153.916
0.838	0.0773	0.0605	0.0156	0.0013	104.708

July 8, 1984
Chuck Site



(a)

July 8, 1984
Chuck Site



(b)

Figure 1. Optical depth versus wavelength data from the Reagan radiometer.

data at 0.872 μm for this date, however, is unreliable, due to the temperature problem mentioned above. With the given constraints, the slope was found to be $a_1 = -0.654$, thus $\nu = 2.65$, and $a_2 = -1.269$. With these constants the τ_{Mie} , τ_{Ray} , and τ_{Oz} components can be computed for any wavelength. Figure 1b shows how each of these components contributes to the total optical depth. Table 2 gives the respective components for the TM midband wavelengths. These data will be used as input to the radiative transfer code. To be complete, a component of $\tau_{\text{H}_2\text{O}}$ should be included for band 4. The contribution due to water vapor has not as yet been assessed. Also reported is the exo-atmospheric solar irradiance, as determined from interpolating the data of Neckel and Labs (1981). The midband wavelengths of the TM sensor was computed by Palmer (1984) using the moments method and the pre-flight filter transmittance data.

Panel Calibration

The Herman radiative transfer code requires that the absolute reflectance of the gypsum sands be known. We have instead chosen to use the reflectance factor $R(\theta_z/0^\circ)$. (A discussion of reflectance nomenclature and definitions is given in Appendix A.) Here θ_z is the angle incident upon the gypsum, and 0° is the reflected angle, equal to the Thematic Mapper nadir-look angle. By using this quantity, the amount of light reflected in the direction of the TM is accurately characterized. A full BRDF characterization would be preferred. The gain in accuracy is not warranted, however, as the BRDF data would be difficult and time consuming to obtain.

In the field the reflectance factor is measured with one of two Barnes radiometers. As these are uncalibrated they must be used in

conjunction with a reference panel. The reflectance factor of the sands is determined via the relationship

$$R_{\text{sand}} = \frac{V_{\text{sand}} * R_{\text{ref}}}{V_{\text{ref}}} . \quad (1)$$

Here V_{sand} and V_{ref} are the output voltages of the Barnes when looking over the sands and reference panel, respectively. These voltages are proportional to the radiance scattered upward and within the instrument's 15° field of view (FOV). R_{ref} is the reflectance factor of the panel, as determined in the laboratory. On July 8th one of the radiometers was assigned the Halon panel; the other radiometer was assigned the BaSO₄ panel. While looking at the sands, each Barnes was periodically swung over the reference panel and voltage readings were recorded. Upon our return Che Nianzeng calibrated both panels.

The calibration of the panels was conducted at the Optical Sciences Center, in a manner illustrated in Figure 2. A tungsten lamp was put at the focal point of an off-axis parabolic mirror. The emerging planar wavefront thereafter illuminated the reference panel at a known angle. The radiance reflected in a direction normal to the surface was then measured using a radiometer built by Che. Thereafter the reference panel was removed, and a primary standard surface put in its place. This primary standard was a Halon panel which had been calibrated by NBS on February 8, 1984. (They determined the reflectance factor $R_{\text{NBS}}(45^\circ/0^\circ)$ for this surface.)

In the first phase of the field panel calibration, the reflectance factor $R_{\text{ref}}(45^\circ/0^\circ)$ was determined. This was computed from the following

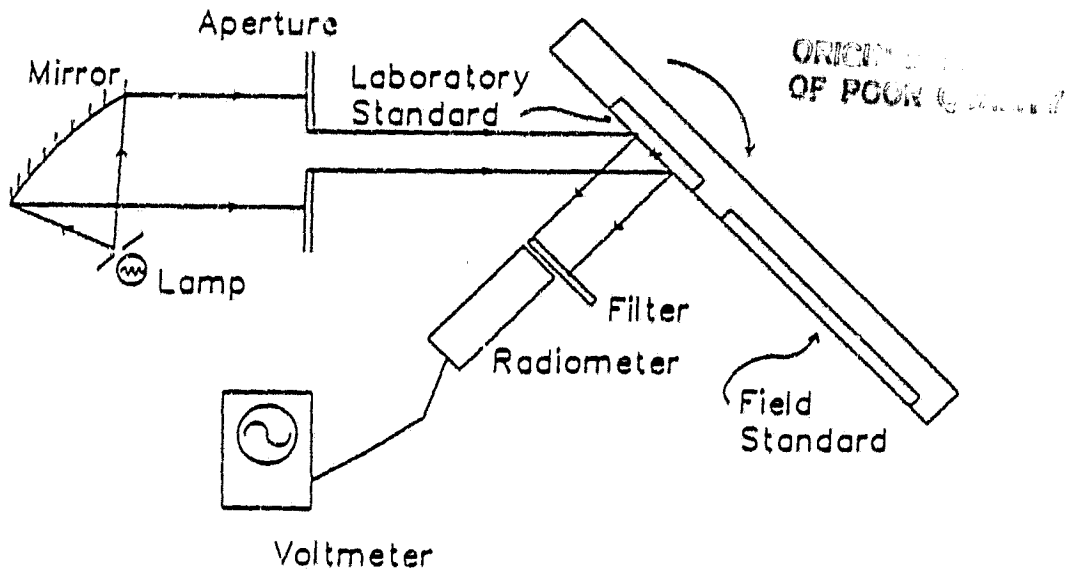


Figure 2. Laboratory set-up for the calibration of field reflectance panels.

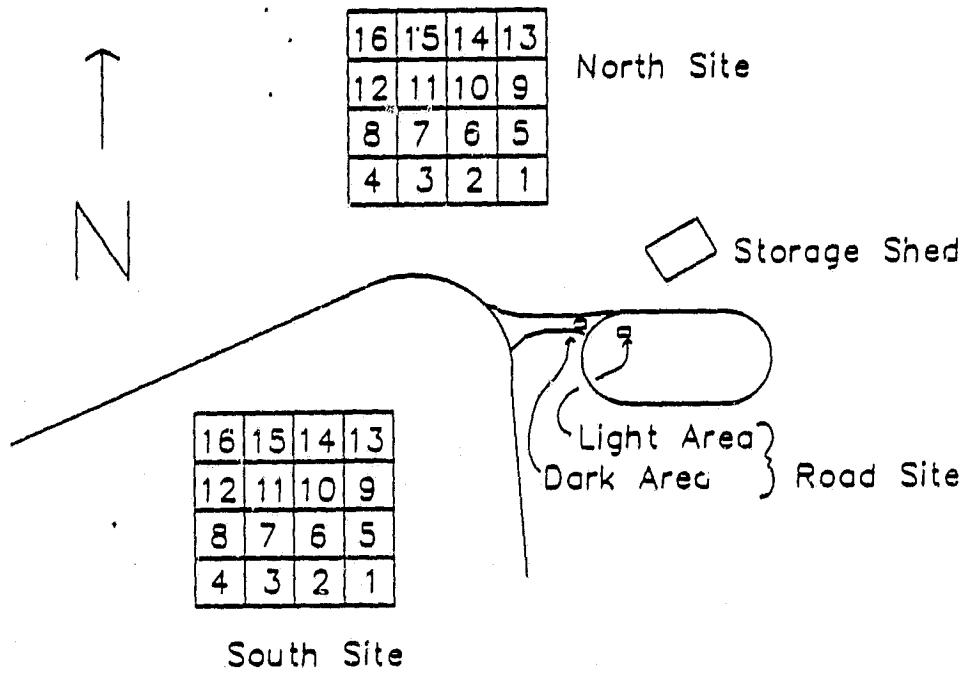


Figure 3. Schematic of Chuck Site test area.

Table 3. Laboratory calibration of BaSO₄ panel.

THE REFLECTANCE FACTOR OF BaSO₄ PANEL NO.5

Irradiance Angle(deg.)	430-470nm	530-570nm	630-670nm	830-870nm
10	1.0420	1.0355	1.0205	0.9858
15	1.0196	1.0138	0.9990	0.9651
20	1.0011	0.9945	0.9807	0.9479
25	0.9836	0.9779	0.9642	0.9331
30	0.9668	0.9610	0.9479	0.9185
35	0.9499	0.9449	0.9327	0.9045
40	0.9326	0.9279	0.9169	0.8905
45	0.9155	0.9119	0.9007	0.8773
50	0.8971	0.8937	0.8851	0.8627
55	0.8783	0.8765	0.8676	0.8474
60	0.8597	0.8582	0.8498	0.8326
65	0.8380	0.8390	0.8310	0.8157
70	0.8157	0.8174	0.8127	0.7986
75	0.7926	0.7929	0.7892	0.7789

Data: July 12, 1984

Sample: BaSO₄ Panel No.5

Reference: Halon calibrated at (45/0) geometry by NBS (Feb.
8, 1984)

Location: Infra. Lab., OSC

Viewing Zenith Angle: 0 deg.

Irradiance Angle: 10-75 deg.

Table 4. Laboratory calibration of Halon panel.

THE REFLECTANCE FACTOR OF HALON PANEL (RAY'S)

Irradiance Angle(deg)	430-470nm	530-570nm	630-670nm	830-870nm
10	0.9965	1.0007	1.0020	1.0042
15	0.9892	0.9949	0.9951	0.9973
20	0.9829	0.9872	0.9888	0.9901
25	0.9741	0.9794	0.9804	0.9816
30	0.9648	0.9702	0.9716	0.9728
35	0.9556	0.9597	0.9618	0.9636
40	0.9442	0.9489	0.9499	0.9515
45	0.9319	0.9368	0.9377	0.9391
50	0.9166	0.9210	0.9231	0.9253
55	0.8991	0.9042	0.9061	0.9073
60	0.8784	0.8832	0.8860	0.8877
65	0.8539	0.8608	0.8633	0.8638
70	0.8221	0.8297	0.8323	0.8343
75	0.7805	0.7872	0.7919	0.7944

Data: July 12, 1984

Sample: Halon panel (Ray's)

Reference: Halon calibrated at (45/0) geometry by NBS (Feb. 8, 1984)

Location: Infra. Lab., OSC

Viewing Zenith Angle: 0 deg.

Irradiance angle: 10-75 deg.

$$R_{\text{ref}}(45^\circ/0^\circ) = \frac{V_{\text{ref}}(45^\circ/0^\circ) * R_{\text{NBS}}(45^\circ/0^\circ)}{V_{\text{NBS}}(45^\circ/0^\circ)} \quad (2)$$

Next, the desired reflectance factor was computed from

$$R_{\text{ref}}(\theta/0^\circ) = \frac{V_{\text{ref}}(\theta/0^\circ) * \cos 45^\circ * R_{\text{ref}}(45^\circ/0^\circ)}{V_{\text{ref}}(45^\circ/0^\circ) * \cos \theta} \quad (3)$$

The above steps were repeated for four spectral bandpass filters, each 40 nm wide. The measurement uncertainty was estimated to be less than 1%. A small error in the reflectance factor was also introduced due to the non-uniformity of the panels. In the field the radiance reflected from the panels was averaged over a larger area. This was due to the 15° FOV, as compared to the 1° FOV of the laboratory radiometer. The results of the panel calibration are shown in Table 3 for the BaSO₄ panel, and in Table 4 for Ray Jackson's Halon panel.

Reflectance Data

Both the Barnes data and the panel calibration data were used to determine the reflectance factors of each of the test sites at White Sands. It is noted that the field measurements were taken at several times throughout the morning. Those data taken closest to the time of the Landsat overpass, 11:07:40 MDT, were used in the radiance computations.

Several interpolations had to be made on the laboratory calibration data. The solar zenith angles were first computed for those times at which a field measurement of the sands was taken. The panel reflectance factors of Tables 3 and 4 were next interpolated to find the corresponding reflectance factors at these angles, for the four spectral filters available on Che's radiometer. These wavelengths differ from

those of the Barnes, therefore one more interpolation was necessary. The intermediate computations were used to compute the reflectances for the eight Barnes' wavelengths. (The Barnes' wavelengths correspond to those of the TM, for bands 1-4.)

The reflectance factors of the gypsum are determined from the above computed panel reflectances via Equation (1) above. A summary of this data reduction is given in Table 5. Only the data in channels 1-4 are used here. Reflectance factors are given for pixels 1-16. A schematic of the site, which identifies these pixels is shown in Figure 3.

Radiative Transfer Computations

The mean reflectance values, given in the bold type of Table 5, were used as input to the radiative transfer code. Also input were the atmospheric components listed in Table 2. The usual model assumptions were made for the aerosols. The maximum, minimum, and incremental radial sizes were 5.02, 0.02, and 0.04 μm , respectively. A refractive index of 1.54-0.01i was assumed. The code was run for both a solar zenith angle of 25° and 35°. The output, given in Table 6, is normalized for an exo-atmospheric solar irradiance of 1. After interpolating the data for a solar angle of 29.22° (that corresponding to the time of the overpass) the output is multiplied by the appropriate irradiance value. These final values are given in Table 7. They are the radiances that were incident on the TM sensor, for the morning of July 8.

Summary

Because of instrumentation problems and difficulties in accurately mapping ground reflectance due to the helicopter photography not being

Table 5. Absolute Reflectance of White Sands test sites.

North Site

TIME	ABSOLUTE REFLECTANCE						
	CH(1)	. . .	CH(7)				
BaSO4							
10:52	.957	.952	.939	.915	.858	.839	.715
11:02	.964	.959	.946	.921	.863	.844	.718
ROAD							
10:54	.510	.577	.619	.650	.625	.527	.259
PIXELS 1-4,8							
10:57	.503	.573	.616	.648	.620	.517	.246
10:57	.510	.581	.627	.660	.632	.527	.236
10:58	.515	.584	.629	.661	.631	.525	.244
10:59	.530	.601	.645	.680	.646	.535	.231
11:01	.504	.571	.617	.652	.629	.526	.231
BASO4							
11:02	.964	.959	.946	.921	.863	.844	.718
11:08	.968	.963	.950	.924	.866	.846	.719
PIXELS 7-5							
11:04	.475	.538	.579	.610	.589	.492	.233
11:05	.488	.552	.594	.626	.601	.497	.230
11:06	.504	.571	.613	.643	.611	.502	.224
BASO4							
11:08	.968	.963	.950	.924	.866	.846	.719
11:15	.973	.968	.954	.929	.869	.849	.719
PIXELS 9-12							
11:08	.488	.555	.599	.630	.605	.501	.230
11:10	.504	.574	.620	.653	.623	.511	.229
11:11	.512	.580	.624	.657	.627	.519	.228
11:12	.526	.597	.643	.676	.637	.520	.213
BASO4							
11:15	.973	.968	.954	.929	.869	.849	.719
11:20	.976	.971	.958	.932	.871	.851	.720
PIXELS 13-16							
11:17	.501	.566	.608	.637	.611	.512	.252
11:18	.533	.602	.644	.674	.640	.533	.225
11:19	.511	.581	.624	.656	.631	.526	.228
11:20	.513	.583	.626	.656	.621	.508	.215
CUMULATIVE:							
MEAN	.507	.576	.619	.651	.622	.516	.231
SDEV	.015	.017	.018	.019	.015	.013	.013

UNCLASSIFIED
OF POOR QUALITY

Table 5. ContinuedORDER
OF POC

South Site

TIME	ABSOLUTE REFLECTANCE						
	CH(1)	CH(2)	CH(3)	CH(4)	CH(5)	CH(6)	CH(7)
Halon							
10:58	.965	.968	.970	.971	.973	.974	.980
11:09	.969	.973	.974	.975	.977	.978	.983
1ST SCAN (PIXELS 1-16)							
10:59	.489	.551	.599	.642	.625	.500	.233
10:59	.494	.557	.601	.638	.618	.497	.241
11:00	.491	.548	.590	.627	.604	.481	.229
11:00	.468	.529	.573	.612	.591	.468	.229
11:01	.487	.546	.588	.626	.600	.480	.246
11:01	.493	.550	.592	.632	.606	.482	.228
11:02	.509	.572	.615	.653	.630	.508	.251
11:02	.514	.576	.618	.658	.628	.500	.231
11:03	.486	.546	.590	.629	.614	.491	.236
11:04	.503	.567	.611	.650	.634	.519	.256
11:04	.516	.578	.622	.660	.637	.512	.243
11:05	.498	.559	.603	.641	.621	.500	.241
11:05	.510	.572	.616	.654	.624	.492	.228
11:06	.510	.569	.610	.647	.616	.489	.230
11:06	.506	.567	.610	.650	.632	.514	.250
11:07	.503	.561	.603	.643	.622	.500	.250
MEAN	.499	.559	.603	.641	.619	.496	.239
SDEV	.013	.014	.013	.013	.013	.014	.010
Halon							
11:16	.972	.975	.976	.977	.980	.980	.986
11:27	.976	.979	.980	.981	.984	.984	.989
2ND SCAN (PIXELS 1-16)							
11:16	.492	.552	.594	.634	.619	.499	.247
11:17	.495	.561	.607	.646	.625	.500	.240
11:17	.494	.557	.601	.638	.616	.488	.236
11:18	.493	.555	.601	.640	.621	.494	.239
11:18	.499	.558	.600	.638	.612	.487	.248
11:19	.512	.573	.618	.659	.633	.503	.235
11:19	.508	.571	.614	.653	.629	.502	.238
11:20	.520	.582	.626	.666	.638	.503	.234
11:21	.501	.563	.610	.651	.633	.505	.242
11:21	.521	.587	.633	.673	.654	.527	.250
11:22	.519	.582	.626	.665	.643	.513	.239
11:22	.518	.579	.623	.662	.642	.517	.249
11:23	.520	.584	.630	.670	.639	.500	.229
11:24	.513	.573	.618	.659	.633	.502	.244
11:24	.507	.573	.618	.658	.640	.520	.254
11:25	.514	.574	.616	.655	.630	.501	.250
MEAN	.508	.570	.615	.654	.632	.504	.242
SDEV	.011	.011	.012	.012	.011	.011	.007

Table 5. Continued

Road Site

TIME	ABSOLUTE REFLECTANCE						
	CH(1)	. . .	CH(7)				
BASO4							
10:27	.940	.935	.924	.900	.846	.828	.711
10:32	.943	.939	.927	.903	.849	.831	.711
1ST DARK AREA							
10:28	.445	.495	.529	.553	.540	.472	.235
10:28	.459	.508	.541	.562	.543	.473	.228
10:28	.463	.513	.544	.565	.543	.470	.223
10:29	.458	.509	.543	.564	.543	.470	.224
10:29	.473	.525	.559	.581	.558	.481	.226
MEAN	.459	.510	.543	.565	.545	.473	.227
SDEV	.010	.011	.011	.010	.007	.005	.005
1ST LIGHT AREA							
10:29	.516	.580	.623	.656	.607	.480	.178
10:30	.501	.560	.600	.632	.585	.463	.169
10:30	.504	.564	.602	.635	.589	.469	.174
MEAN	.507	.568	.608	.641	.594	.471	.174
SDEV	.008	.010	.013	.013	.012	.009	.004
BASO4							
10:37	.947	.942	.930	.906	.851	.832	.712
10:40	.949	.944	.932	.908	.852	.834	.712
2ND DARK AREA							
10:37	.447	.495	.527	.549	.534	.467	.233
10:38	.455	.505	.538	.559	.543	.473	.233
10:38	.457	.506	.538	.560	.541	.469	.224
10:38	.457	.507	.540	.562	.541	.467	.224
10:38	.476	.525	.558	.579	.556	.476	.223
MEAN	.458	.508	.540	.562	.543	.470	.227
SDEV	.011	.011	.011	.011	.008	.004	.005
2ND LIGHT AREA							
10:39	.516	.578	.618	.651	.604	.477	.177
10:39	.505	.566	.605	.638	.590	.463	.167
10:40	.504	.561	.597	.628	.583	.464	.172
MEAN	.509	.568	.607	.639	.592	.468	.172
SDEV	.007	.009	.011	.011	.010	.008	.005
BASO4							
11:38	.989	.983	.969	.942	.879	.859	.722
11:42	.991	.986	.972	.945	.881	.860	.723

Road Site. Continued

ORIGINAL I. I.
OF POOR QUALITY

3RD DARK AREA

11:39	.478	.534	.568	.589	.569	.495	.245
11:39	.479	.534	.569	.591	.567	.488	.233
11:40	.487	.543	.577	.598	.573	.493	.236
11:40	.485	.542	.577	.598	.571	.490	.233
11:40	.499	.554	.587	.608	.580	.495	.232
MEAN	.486	.541	.576	.597	.572	.492	.236
SDEV	.008	.008	.008	.008	.005	.003	.005

3RD LIGHT AREA

11.41	.540	.608	.651	.682	.629	.498	.189
11.41	.530	.597	.639	.669	.614	.481	.176
11.42	.530	.598	.639	.667	.613	.485	.181
MEAN	.533	.601	.643	.673	.619	.488	.182
SDEV	.006	.006	.007	.008	.009	.009	.006

Table 6. Herman Code Output

WAV	τ_{Mie}	τ_{Ray}	τ_{oz}	θ_z	ρ	E _{dir}	E _{dif}	L _{path}	L _t
0.486	0.0864	0.1421	0.0055	25	0.507	0.7001	0.1519	0.0246	0.1334
					0.499				
0.486	0.0864	0.1421	0.0055	35	0.507	0.6156	0.1417	0.0223	0.1190
					0.499				
0.571	0.0777	0.0735	0.0232	25	0.576	0.7477	0.1113	0.0134	0.1457
					0.559				
0.571	0.0777	0.0735	0.0232	35	0.576	0.6621	0.1028	0.0121	0.1299
					0.559				
0.661	0.0706	0.0406	0.0114	25	0.619	0.7916	0.9078	0.0080	0.1618
					0.603				
0.661	0.0706	0.0406	0.0114	35	0.619	0.7053	0.8337	0.0072	0.1447
					0.603				
0.838	0.0605	0.0156	0.0013	25	0.651	0.8321	0.6780	0.0033	0.1759
					0.641				
0.838	0.0605	0.0156	0.0013	35	0.651	0.7453	0.6182	0.0030	0.1578
					0.641				

where

E_{dir} The downward direct solar irradiance at the ground, $\cos\theta_z$ * $\exp(-\tau_{ext} \sec\theta_z)$.

E_{dif} The downward diffuse solar irradiance at the ground.

L_{path} The upward path radiance at the TM, $L_T - (E_{dir} + E_{dif}) * \exp(-\tau_{ext} \sec 5^\circ) \rho / \pi$

L_t The total radiance at the TM at a 5° nadir angle.

Note all irradiance and radiance values are normalized for an exo-atmospheric solar irradiance of 1.

Table 7. Computed radiance at Landsat sensors.

Band	L (mW/cm ² sr μm)	
	North Site	South Site
1	23.18	22.82
2	25.13	24.37
3	23.82	23.17
4	17.64	17.35

vertical, the results of the July 8, 1984 measurement will have high uncertainties associated with them. However, the measurement attempt was worthwhile because of the experience gained in instrument operation and measurement.

There are still a few remaining computations to be made with the July 8th data. Only a few discrete points of data were taken at the pixel centers of the two test sites. We are currently exploring the usage of the aerial photography (the slide imagery which has been scanned) to better characterize the reflectance of the area. The radiosonde and humidity data will also be looked at. Once the optical depth component τ_{H_2O} can be determined, the Herman code will be rerun to account for atmospheric water vapor in band 4. The diffuse to direct data will be compared with the Herman code output. Finally, it remains to inspect the Landsat imagery, identify our test site, and compute incident radiance, as determined from the pre-flight data. A comparison can then be made of our in-flight calibration, to that made based upon pre-flight data and the internal calibrator data. The calibrations of bands 5 and 7 will not be investigated for this date. No atmospheric data are available at these wavelengths and the optical depth components cannot be computed. The Castle spectropolarimeters will be equipped with a filter set which will allow us, in the future, to do calibrations in the short wave infrared.

References

1. Neckel, H. and D. Labs. "Improved data of solar spectral irradiance from 0.33 to 1.25 μm ". Solar Physics, Vol. 74, p. 231, 1981.
2. Palmer, James M. "Effective bandwidths for Landsat-4 and Landsat-4' multispectral scanner and thematic mapper subsystems". IEEE trans, Geoscience and Remote Sensing, Vol. GE-22, p.336-338, 1984.

APPENDIX A

Reflectance

The nomenclature, measuring geometry, and techniques associated with determining the reflectance of a given surface are quite varied. With this in mind, the technical basis of our measurements at White Sands is presented here. We are interested in the directional properties, as well as the magnitude, of the reflectance at the field site, for this reason we determine the reflectance factor. Reflectance factor and other quantities are defined below. A spectral dependence is assumed for each quantity. All of our reflectance measurements are made with finite spectral bandwidths. These are, in general, the 40 nm bandwidths of a laboratory radiometer, or those bandwidths associated with the Thematic Mapper and the Barnes modular multiband radiometer.

Definitions and Nomenclature

Reflectance Factor, $R(\theta, \phi; \theta', \phi')$ (unitless). Ratio of the flux reflected by a sample surface to that which would be reflected into the same beam geometry by a lossless, lambertian surface which is identically irradiated. Thus,

$$R(\theta, \phi; \theta', \phi') = \frac{\int_{\text{IFOV}} L_t(\theta', \phi') \cos \theta' \sin \theta' d\theta' d\phi'}{\int_{\text{IFOV}} L_p(\theta', \phi') \cos \theta' \sin \theta' d\theta' d\phi'} \quad (1)$$

is the reflectance factor measured with a detector having a given

instantaneous field of view (IFOV). L_t is the radiance reflected off the sample target, and L_p is the radiance reflected off a perfect (lossless), diffuse surface. The incident beam originates from (θ, ϕ) , and the reflected beam is viewed in the direction (θ', ϕ') .

Reflectance ρ (unitless). Ratio of the reflected flux to the incident flux. When referring to this parameter one needs to specify if the flux is integrated over the reflecting hemisphere, or if the reflected flux is measured within a given cone angle. The hemispherical reflectance can be related to the reflectance factor by

$$\rho = \int_{2\pi} \int_{\pi/2} L_t(\theta', \phi') \cos\theta' \sin\theta' d\theta' d\phi' / E \quad (2)$$

$$= R(\theta, \phi; 2\pi)$$

where E is the incident irradiance, generally from a well collimated beam. It is computed from

$$E = \int \int_{\omega} L_t(\theta, \phi) \cos\theta \sin\theta d\theta d\phi \quad (3)$$

Note the integration is over the solid angle $d\omega = \sin\theta d\theta d\phi$.

Bidirectional Reflectance Distribution Function (BRDF), f (sr^{-1}). The ratio of the radiance reflected in the direction (θ', ϕ') to the total irradiance on the surface from the direction (θ, ϕ) .

$$f(\theta, \phi; \theta', \phi') = L_t(\theta', \phi') / E \quad (4)$$

The quantity $R(\theta, \phi; 2\pi)$ is equivalent to ρ . The 2π denotes that the reflectance factor has been integrated over a hemisphere. $R(\theta; d)$, or $R(\theta/d)$, is an equivalent description, the "d" denoting that diffuse reflectance has been accounted for. Even when an integration is not

implied, the symbols ϕ and ϕ' are often dropped for simplicity (as is true for any of the above parameters).

Choice of the Reflectance Factor

In calibrating the TM we are interested in knowing the radiance reflected from the gypsum sands into a number of discrete angles. This allows both the directly and diffusely reflected solar radiation to be accurately characterized. Such a complete BRDF measurement is, however, both time consuming and difficult to measure. The equipment required is relatively complex, and there are difficulties associated with measuring the incident irradiance. Instead we have chosen to characterize the gypsum by the reflectance factor $R(\theta_z; 0^\circ)$. This accurately describes the flux that is directly reflected towards the Landsat sensors. As the gypsum sands are not truly lambertian, some error is incurred in not computing the full BRDF. Without the BRDF data, a lambertian surface is assumed. Thus an overestimate is made in the radiance not directly reflected towards the TM. Due to atmospheric multiple scattering in the atmosphere, some of this flux eventually reaches the sensors. This is the diffuse component of the radiance. The error made in predicting this term increases with increased multiple scattering, and with departure from a lambertian behavior. Even so, the usage of the reflectance factor is justified. This is because the radiance received at the TM is dominated by the direct component, and multiple scattering is minimal for clear atmospheric conditions.

Calibrating the Field Reference

The reflectance factor is measured with respect to a reference panel which is calibrated in the laboratory to account for its non-ideal characteristics. The calibration procedure was briefly described in the body of the report. Here a development of the equations used in the two step calibration procedure is given.

To begin with, it is assumed that a laboratory standard is available. In our case a 50 mm diameter Halon disc was used which had been calibrated by NBS to determine $R_{NBS}(45^\circ;0^\circ)$. The fictional parameter $V_p(45^\circ;0^\circ)$ is thereby computed:

$$V_p(45^\circ;0^\circ) = \frac{V_{NBS}(45^\circ;0^\circ)}{R_{NBS}(45^\circ;0^\circ)} \quad (5)$$

This is the voltage that would have been measured had a perfect (lossless) lambertian surface been present.

Using the above, the reflectance factor of the reference panel is found for the same geometry:

$$\begin{aligned} R_{ref}(45^\circ;0^\circ) &= \frac{V_{ref}(45^\circ;0^\circ)}{V_p(45^\circ;0^\circ)} \\ &= \frac{V_{ref}(45^\circ;0^\circ) * R_{NBS}(45^\circ;0^\circ)}{V_{NBS}(45^\circ;0^\circ)} \end{aligned} \quad (6)$$

In the next phase of calibration, the reflectance factor measurements are made at the angle of interest, θ . For the ideal lambertian surface the detector response at angle θ is easily predicted from the response at 45° . Such a surface reflects radiance uniformly into the upper hemisphere, thereby reflecting a factor of $1/\pi$ of the incident irradiance. Thus, for this perfect ($\rho=1$) lambertian surface, illuminated with a beam of irradiance $E(\theta)$, the following relationships

hold:

$$V_p(45^\circ; 0^\circ) = R * E(45^\circ) \rho / \pi = R * E_0 \cos 45^\circ / \pi \quad (7)$$

$$\begin{aligned} V_p(\theta; 0^\circ) &= R * E(\theta) \rho / \pi = R * E_0 \cos \theta / \pi \quad (8) \\ &= \frac{V_p(45^\circ; 0^\circ) * \cos \theta}{\cos 45^\circ} \end{aligned}$$

The detector is assumed to have a given response, R, to the incoming radiance. This latter result is now substituted into the equation for $R_{ref}(\theta; 0^\circ)$, to yield the final, desired result:

$$\begin{aligned} R_{ref}(\theta; 0^\circ) &= \frac{V_{ref}(\theta; 0^\circ)}{V_p(\theta; 0^\circ)} \quad (9) \\ &= \frac{V_{ref}(\theta; 0^\circ) * \cos 45^\circ}{V_p(45^\circ; 0^\circ) * \cos \theta} \\ &= \frac{V_{ref}(\theta; 0^\circ) * \cos 45^\circ * R_{ref}(45^\circ; 0^\circ)}{V_{ref}(45^\circ; 0^\circ) * \cos \theta} \end{aligned}$$

APPENDIX B

Radiosonde and atmospheric data for July 8th, as provided by the
Atmospheric Sciences Laboratory, White Sands Missile Range.

PROJECT SURFACE OBSERVATION

MISSION CODE LANDSAT 5

STATION CHUCK SLIF

DATE 08 07 84
DAY MONTH YEAR

X= 32° 54' Y= 106° 18' H= 3912.75f

TIME M D J	PRESSURE mbs	TEMPERATURE °F	TEMPERATURE °C	DEW POINT OF	RELATIVE HUMIDITY %	DENSITY gm/m ³	WIND		VISIBIL- ITY
							DIRECTION degs In	SPEED kts	
0730	883.8	68.4	20.2	54.3	61	1042	105	01	40
0930	883.4	81.0	27.2	56.1	42	1019	095	01	40
0945	883.4	83.3	28.5	55.2	38	1015	100	01	40

OBSTRUCTIONS TO VISIBILITY	CLOUDS						REMARKS		
	1st LAYER		2nd LAYER		3rd LAYER				
	AMT	HGT	AMT	HGT	AMT	HGT			
						1	Ci	25000	
						2	Ci	25000	
						2	Ci	25000	

PSYCHROMETRIC COMPUTATION

TIME:	0730	0930	0945
DRY BULB TEMP.	20.2	27.2	28.5
WET BULB TEMP.	15.2	18.0	18.1
WET BULB DEPR.	5.0	9.2	10.4
DEW POINT	12.4	13.4	12.9
RELATIVE HUMID.	61	42	38

ORIGINAL PAGE IS
OF POOR QUALITY

R. Savage
OBSERVER

VERIFIER

PROJECT SURFACE OBSERVATION

MISSION CODE LANDSAT-5

STATION CHUCK SITE

DATE 08 07 84
DAY MONTH YEAR

$\lambda =$ 32°54' $\gamma =$ 106°18' $H =$ 3012.75ft

TIME M D I	PRESSURE inbs	TEMPERATURE OF °C	DEW POINT OF °C	RELATIVE HUMIDITY %	DENSITY gm/m ³	WIND		VISIBIL- ITY
						DIRECTION degs In	SPEED kts	
1000	883.3	84.4	29.1	37	1012	090	02	40
1015	883.2	86.0	30.0	40	1009	095	03	40
1030	883.2	86.4	30.2	40	1008	080	05	40

OBSTRUCTIONS TO VISIBILITY	CLOUDS						REMARKS		
	1st LAYER		2nd LAYER		3rd LAYER				
	AMT	TYPE	HGT	AMT	TYPE	HGT			
	1	Cu	6000	0	AC	12000	2	Ci	25000
	1	Cu	6000	0	AC	12000	2	Ci	25000
	2	Cu	6000	0	AC	12000	2	Ci	25000

UNACCEPTABLE
OF POOR QUALITY

PSYCHROMETRIC COMPUTATION

TIME:	1000	1015	1030
DRY BULB TEMP.	29.1	30.0	30.2
WET BULB TEMP.	18.3	19.7	19.8
WET BULB DEPR.	10.8	10.3	10.4
DEW POINT	12.9	15.0	15.1
RELATIVE HUMID.	37	40	40

A. Savage
OBSERVER

VERIFIER

PROJECT SURFACE OBSERVATION

MISSION CODE LANDSAL-5

STATION CHUCK SITE

DATE 08 07 84 YEAR
DAY MONTH YEAR

X= 32°54' Y= 106°18' H= 3912.75ft

TIME M D I	PRESSURE mbs	TEMPERATURE OF °C	DEW POINT OF °C	RELATIVE HUMIDITY %	DENSITY gm/cm ³	WIND		VISIBIL- ITY
						DIRECTION degs	SPEED kts	
1045	883.2	30.5	58.8	39	1007	095	04	40
1100	883.1	31.3	58.5	36	1005	095	04	40
1107	883.0	32.2	57.9	34	1002	100	04	40

OBSTRUCTIONS TO VISIBILITY	CLOUDS						REMARKS
	1st LAYER		2nd LAYER		3rd LAYER		
	AMT	HTGT	AMT	HTGT	AMT	HTGT	
	2	Cu 6000	0	AC 12000	2	Ci 25000	
	2	Cu 6000	0	AC 12000	2	Ci 25000	
	2	Cu 6000	0	AC 12000	2	Ci 25000	

PSYCHROMETRIC COMPUTATION

TIME:	1045	1100	1107
DRY BULB TEMP.	30.5	31.3	32.2
WET BULB TEMP.	19.8	19.9	20.0
WET BULB DEPR.	10.7	11.4	12.2
DEW POINT	14.9	14.7	14.4
RELATIVE HUMID.	39	36	34

R. Savage
OBSERVER

VERIFIER

PROJECT SURFACE OBSERVATION

MISSION CODE LANDSAT-5 STATION CHUCK SITE

DATE 08 07 84 X = 32°54' Y = 106°18' H = 3912.75ft
 DAY MONTH YEAR

TIME M D I	PRESSURE mbs	TEMPERATURE OF °C	DEW POINT OF °C	RELATIVE HUMIDITY %	DENSITY gm/m ³	WIND		VISIBIL- ITY		
						DIRECTION degs In	SPEED kts			
1115	882.9	92.1	33.4	57.6	14.2	31	998	100	03	40
1130	882.8	95.0	35.0	57.0	13.9	28	993	095	04	40

OBSTRUCTIONS TO VISIBILITY	CLOUDS						REMARKS			
	1st LAYER		2nd LAYER		3rd LAYER					
	AMT	TYPE	HGT	AMT	TYPE	HGT				
	2	Cu	6000	0	AC	12000	2	Ci	25000	
	2	Cu	6000	0	AC	12000	2	Ci	25000	

ORIGINAL FORM OF POOR QUALITY

PSYCHROMETRIC COMPUTATION

TIME:	1115	1130
DRY BULB TEMP.	33.4	35.0
WET BULB TEMP.	20.2	20.5
WET BULB DEPR.	13.2	14.5
DEW POINT	14.2	13.9
RELATIVE HUMID.	31	28

R. Sarge

OBSERVER

VERIFIER

SYNTHETIC COORDINATES
 32.43063 LAT DEG
 106.37033 LON DEG

ORIGINAL PAGE IS
 OF POOR QUALITY

STATION NAME
 100070105
 WHITE SANDS

STAT ALTITUDE 207.0 FEET ASL
 2 JULY 54
 ASCENSION NO. 255

PRESSURE MILLIBARS	GEOCENTRIC ALTITUDE MSL FEET	TEMPERATURE		REL. HUM. PERCENT
		AIR DEGREES CENTIGRADE	DEW POINT CENTIGRADE	
21.0	3499.0	25.0	12.2	43.0
271.1	4215.5	24.3	3.7	37.0
500.0	5012.7	22.7	7.1	62.0
725.1	5217.2	20.0	7.4	44.0
747.1	5071.9	15.8	5.1	49.0
725.5	5432.5	14.0	2.7	47.0
237.0	12472.2	11.5	2.5	54.0
201.9	11174.7	9.3	1.7	50.0
451.2	12415.9	6.7	-0.4	52.0
334.0	17144.3	4.0	-1.6	57.0
415.4	17916.2	3.2	-10.4	36.0
407.7	14274.9	3.0	-14.5	25.0
564.3	15351.0	1.5	-15.0	23.0
358.3	16379.4	.1	-20.7	19.0
515.7	18541.4	-4.5	-74.6	17.0
500.0	17477.2	-7.1	-26.7	19.0
475.8	27025.7	-7.3	-23.1	17.0
400.0	25044.3	-17.0	-24.1	21.0
743.5	27744.0	-24.4	-40.8	20.0
100.0	31941.0	-33.3	-43.0	21.0
200.2	37510.5	-35.4	-50.7	21.0
264.3	34830.5	-37.2	-52.0	24.0
250.0	36270.9	-62.9		
221.3	38354.4	-49.1		
267.0	40911.8	-53.9		
170.2	44273.2	-50.7		
120.0	44245.7	-64.0		
133.7	42729.5	-57.8		
119.2	51413.1	-70.3		
100.0	54242.5	-71.2		
55.2	58032.5	-53.8		
70.2	67074.1	-54.7		
54.5	58225.4	-51.3		
57.0	59722.5	-55.7		
64.4	71203.3	-55.1		
55.2	75244.4	-52.8		
57.0	79271.3	-52.4		
24.0	84441.6	-51.7		
29.0	84225.3	-46.1		
10.6	22559.2	-62.5		

STATION ALTITUDE 5759.0 FEET MSL
6 JULY 64
ASCENSION MD. 356
LSCC HAS MST

SIGNIFICANT LEVEL DATA

1000 FT
WHITE SANDS

GEODETIC COORDINATES
32.63043 LAT NEG
106.37053 LONG DEG

PRESSURE GEOMETRIC
ALTITUDE
MILLIBARS MEL FEET

12.6 27171.1

TEMPERATURE
AIR DEGREE
DEGREES CENTIGRADE

-49.1

REL. HUM.
PERCENT

ORIGINAL
OF POON

ORIGINAL PAGE
OF POOR QUALITY

GEODETIC COORDINATES
32.43063 LAT DES
106.57255 LON DEG

UPPER AIR DATA
1000Z0306
WHITE SANDS

STATION ALTITUDE 5255.0 FEET MSL
2 JULY 84
0850 HRS MST
ASCENSION NO. 350

GEOMETRIC ALTITUDE MSL FEET	PRESSURE MILLIBARS	TEMPERATURE AIR DEGREES CELSIUS	REF. HUM. PERCENT	DENSITY GM/CM ³ AFTER	SPEED OF WIND KNOTS	WIND DATA		INDEX OF REFRACTION
						DIRECTION DEGREES(T)	SPEED (KNOTS)	
5255.0	551.0	26.9	41.0	1016.5	575.9	7	0	1.0002225
4700.0	600.7	26.6	49.9	1016.5	676.2	170.0	.1	1.0002285
4500.0	655.5	23.9	38.3	1010.1	573.1	170.7	2.5	1.0002274
3970.0	675.0	22.7	41.9	974.2	571.9	170.9	5.7	1.0002272
3500.0	575.0	22.0	42.5	951.4	671.0	170.9	10.4	1.0002265
3000.0	621.2	21.5	43.0	954.7	570.2	191.5	11.7	1.0002263
2500.0	600.8	20.6	43.6	952.2	657.4	192.4	11.6	1.0002259
2000.0	724.2	19.0	44.2	938.2	658.4	195.0	9.6	1.0002254
1500.0	776.9	18.0	45.7	925.5	557.0	201.7	7.5	1.0002250
1000.0	765.2	17.4	47.1	917.1	565.0	204.5	7.4	1.0002245
500.0	751.7	15.2	45.5	906.7	554.2	206.5	7.1	1.0002241
000.0	728.3	15.1	48.2	856.5	552.3	206.1	5.6	1.0002235
950.0	735.2	14.0	47.1	874.4	661.4	175.5	4.9	1.0002230
1000.0	712.2	12.7	50.5	854.5	550.0	165.2	3.4	1.0002227
1050.0	699.4	11.4	54.2	857.8	653.5	123.4	4.9	1.0002224
1100.0	650.0	9.9	58.4	841.2	555.7	105.4	7.2	1.0002221
1150.0	674.3	9.9	56.5	830.7	555.1	74.5	8.9	1.0002217
1200.0	672.0	7.3	51.3	819.3	553.6	39.1	10.7	1.0002213
1250.0	649.9	5.0	52.5	808.1	552.1	84.1	12.3	1.0002209
1300.0	627.9	4.5	55.9	797.7	550.2	35.3	13.6	1.0002205
1350.0	626.1	3.6	57.2	726.0	549.0	88.3	16.8	1.000196
1400.0	614.5	3.2	33.8	773.5	548.1	72.1	14.2	1.000185
1450.0	603.0	2.7	26.4	750.5	547.4	98.7	13.5	1.000174
1500.0	591.8	2.0	27.3	748.3	545.6	108.4	13.2	1.000175
1550.0	580.7	1.5	20.9	756.2	545.5	118.4	13.5	1.000173
1600.0	569.1	.7	23.1	724.1	645.0	127.2	16.9	1.000169
1650.0	558.1	.1	19.3	712.1	544.3	133.4	15.0	1.000165
1700.0	548.0	.7	19.0	701.5	543.0	138.0	15.9	1.000162
1750.0	573.1	2.1	19.0	691.1	541.6	141.6	15.4	1.000159
1800.0	527.9	3.2	19.0	630.2	540.3	144.9	14.5	1.000155
1850.0	517.2	4.4	19.0	670.8	638.2	146.4	13.1	1.000154
1900.0	508.0	5.6	14.0	661.7	537.1	145.5	13.6	1.000151
1950.0	490.2	7.1	16.2	652.1	635.6	144.5	14.7	1.000149
2000.0	445.2	7.2	18.0	659.7	525.5	148.7	15.5	1.000146
2050.0	479.1	7.3	17.2	627.5	525.6	152.7	15.5	1.000143
2100.0	465.8	5.1	17.2	617.2	624.4	157.3	17.7	1.000141
2150.0	460.5	7.0	17.5	607.5	523.0	160.4	18.9	1.000139
2200.0	451.5	10.5	15.2	599.1	621.7	162.4	19.6	1.000135
2250.0	442.0	11.4	15.7	528.3	520.4	162.8	17.5	1.000134
2300.0	433.0	12.5	15.1	579.7	523.1	151.9	18.4	1.000132

ORIGINAL PAGE IS
OF POOR QUALITY

STATION ALTITUDE - 200.00 FEET MSL
1 JULY 64
ASCENSION 010. 250

UPPER AIR DATA
1000023100
WHITE SANDS

GEODETIC COORDINATES
32.63063 LAT DEG
106.37933 LON DEG

GEOGRAPHIC ALTITUDE MSL FEET	PRESSURE MILLIBARS	TEMPERATURE AIR DEGREES CELSIUS	REL. HUM. PERCENT	DENSITY GM/CM ³ METER	SPEED OF SOUND		WIND DATA		INDEX OF REFRACTION
					KNOTS	KNOTS	DIRECTION DEGREES(TVD)	SPEED KNOTS	
205.00	4.30	-31.9	19.6	570.7	527.7	159.7	17.4	1.000127	
240.00	4.17	-32.0	20.1	569.2	526.4	156.9	17.0	1.000127	
245.00	4.05	-33.3	20.5	557.1	525.1	157.5	15.2	1.000125	
250.00	3.92	-34.0	21.0	544.5	523.7	153.4	15.4	1.000123	
255.00	3.80	-34.9	20.9	535.7	522.5	150.0	14.1	1.000121	
260.00	3.68	-35.8	20.5	524.3	521.3	149.4	13.2	1.000119	
265.00	3.56	-36.7	20.5	518.2	520.0	149.1	12.2	1.000117	
270.00	3.44	-37.5	20.5	507.7	518.3	148.0	13.7	1.000115	
275.00	3.31	-38.5	20.3	501.2	617.6	148.9	15.4	1.000113	
280.00	3.18	-39.5	20.2	493.1	515.3	148.3	11.5	1.000111	
285.00	3.07	-40.4	20.1	485.0	515.1	147.3	9.2	1.000109	
290.00	2.95	-41.4	20.1	477.3	613.6	142.5	7.7	1.000107	
295.00	2.82	-42.5	20.2	469.2	511.2	136.1	5.3	1.000105	
300.00	2.70	-43.5	20.4	462.7	610.1	127.9	6.0	1.000103	
305.00	2.58	-44.8	20.5	455.5	608.4	115.5	3.8	1.000102	
310.00	2.46	-45.7	20.7	448.5	505.7	95.5	2.9	1.000101	
315.00	2.34	-47.0	20.7	441.7	604.2	72.5	3.7	1.000099	
320.00	2.22	-48.1	21.0	434.3	503.2	91.1	6.9	1.000097	
325.00	2.10	-49.0	21.0	427.2	602.0	32.3	5.2	1.000095	
330.00	1.98	-49.8	21.0	419.7	500.7	75.9	7.4	1.000094	
335.00	1.86	-50.7	21.0	412.4	599.5	59.1	9.0	1.000092	
340.00	1.74	-51.2	22.1	405.5	597.5	56.9	7.7	1.000091	
345.00	1.62	-52.0	23.2	399.0	595.2	52.1	9.5	1.000089	
350.00	1.50	-53.2	21.3**	392.6	594.6	55.8	9.9	1.000088	
355.00	1.38	-53.9	11.6**	385.3	593.0	43.8	3.0	1.000085	
360.00	1.26	-54.9	1.6**	379.3	591.6	24.4	9.8	1.000084	
365.00	1.14	-44.0		372.9	589.9	9.5	11.5	1.000083	
370.00	1.02	-45.2		366.1	588.2	5.1	13.7	1.000082	
375.00	0.90	-46.5		360.1	585.5	7.7	15.6	1.000080	
380.00	0.78	-47.7		354.2	584.9	2.5	15.0	1.000079	
385.00	0.66	-49.0		347.3	583.3	1.1	15.5	1.000077	
390.00	0.54	-50.0		341.4	582.0	359.7	13.7	1.000076	
395.00	0.42	-51.0		335.1	580.6	357.1	20.6	1.000075	
400.00	0.30	-52.0		328.3	579.3	356.7	21.6	1.000073	
405.00	0.18	-53.1		322.7	578.0	356.9	20.2	1.000072	
410.00	0.06	-54.1		316.7	575.5	358.9	17.0	1.000071	
415.00		-55.1		310.5	575.3	3.6	13.8	1.000069	
420.00		-56.1		304.7	574.0	11.2	10.7	1.000068	
425.00		-57.1		298.3	572.5	7.9	9.6	1.000067	
430.00		-58.1		292.1	571.3	1.5	3.9	1.000065	

** AT LEAST ONE ASSUMED RELATIVE HUMIDITY VALUE WAS USED IN THE INTERPOLATION.

STATION ALTITUDE 89,700 FEET MSL
 1 JULY 84
 UBCP HAS MST
 ASCENSION NO. 356

UPPER AIR DATA
 1000Z0366
 WHITE SANDS

GEODETIC COORDINATES
 32.60043 LAT DEG
 136.57053 LON DEG

ORIGINAL PAGE 17
 OF POOR QUALITY

GEOGRAPHIC ALTITUDE MSL FEET	PRESSURE MILLIBARBS	TEMPERATURE AIR DEGREES CENTIGRADE	REL. HUM. PERCENT	DENSITY GM/CM ³ AFTER	SPEED OF SOUND KNOTS	DIRECTION DEGREES(TV)	WIND DATA		INDEX OF REFRACTION:
							SPEED KNOTS	SPEED KNOTS	
45000.0	176.6	-59.1		297.5	559.9	746.9		8.6	1.000044
44000.0	172.1	-59.1		297.0	559.5	731.9		9.0	1.000043
44000.0	170.3	-61.0		276.4	557.4	724.7		10.9	1.000042
43000.0	164.5	-61.0		270.5	555.5	724.8		12.7	1.000063
42500.0	150.2	-62.3		264.7	565.7	742.2		13.9	1.000059
42000.0	155.4	-62.9		250.1	554.9	750.7		14.6	1.000058
40500.0	151.0	-63.6		253.5	554.0	77.5		14.9	1.000055
37500.0	142.8	-64.1		249.2	563.1	32.0		14.6	1.000055
37500.0	145.2	-65.1		247.0	552.0	45.8		14.2	1.000056
36500.0	141.6	-65.7		238.0	550.9	56.3		13.7	1.000053
34500.0	135.1	-66.7		237.0	559.5	67.4		13.6	1.000052
32000.0	134.7	-67.5		228.1	553.7	73.5		11.7	1.000051
31500.0	131.3	-68.1		227.2	557.8	81.0		9.8	1.000050
30000.0	128.1	-68.7		219.2	557.0	84.7		7.8	1.000049
30500.0	134.8	-69.3		217.3	555.3	92.0		6.3	1.000043
31000.0	121.7	-69.6		208.5	555.5	104.5		5.9	1.000046
31500.0	118.7	-70.5		207.3	554.8	112.9		7.8	1.000045
32000.0	115.7	-70.5		195.8	554.7	115.3		9.6	1.000046
32500.0	112.8	-70.0		192.9	554.5	116.9		11.0	1.000045
33000.0	109.9	-70.7		159.1	554.3	115.6		11.6	1.000042
33500.0	107.1	-70.8		184.5	554.1	116.8		12.2	1.000041
34000.0	104.4	-71.0		170.9	553.9	115.3		12.8	1.000040
34500.0	101.3	-71.1		175.5	553.8	115.9		13.5	1.000039
35000.0	99.1	-70.0		170.9	554.1	117.7		16.9	1.000039
35500.0	96.3	-69.7		155.7	555.7	119.7		15.1	1.000037
36000.0	94.4	-68.5		160.7	557.3	120.5		15.5	1.000035
36500.0	92.0	-67.4		155.8	558.9	122.0		15.0	1.000035
37000.0	89.7	-66.2		151.1	549.4	123.0		14.2	1.000034
37500.0	87.1	-65.0		146.5	552.0	124.0		13.3	1.000033
38000.0	85.2	-63.9		142.1	543.6	125.2		11.6	1.000032
38500.0	82.3	-62.9		138.5	553.5	124.5		9.8	1.000031
39000.0	79.2	-64.0		135.3	543.4	102.1		7.7	1.000030
39500.0	75.2	-64.1		132.1	543.2	75.2		7.8	1.000029
40000.0	72.4	-64.2		128.9	553.1	75.2		13.1	1.000029
40500.0	70.4	-64.4		125.8	562.9	77.1		18.3	1.000025
41000.0	70.0	-64.5		123.3	562.6	63.4		21.0	1.000027
41500.0	71.2	-64.0		118.9	562.0	38.9		25.6	1.000027
42000.0	70.0	-64.7		117.0	552.5	94.1		24.9	1.000025
42500.0	68.2	-64.2		113.9	553.1	100.3		24.6	1.000025
43000.0	65.6	-63.8		110.2	563.7	103.5		24.5	1.000025

ORIGINAL PAGE IS
OF POOR QUALITY

SECTETIC COORDINATES
32.6J063 LAT DEG
136.37033 LON DEG

UPPER AIR DATA
1000 20355
WHITE SANDS

STATION ALTITUDE 2549.00 FEET MSL
5 JULY 54
OFFIC HRS 531
ASCENSION NO. 256

GLOMETRIC ALTITUDE MSL FEET	PRESSURE MILLIBARS	TEMPERATURE AIR DEGREES CENTIGRADE	REL. HUM. PERCENT	DENSITY GM/CUBIC METER	SPEED OF SOUND KNOTS	DIRECTION DEGREES(TN)	WIND DATA SPEED (KNOTS)	INDEX OF REFRACTION
63500.0	65.0	-65.3		108.3	564.3	105.2	24.5	1.000024
64000.0	63.4	-62.7		105.1	556.9	106.1	24.7	1.000023
64500.0	61.9	-62.4		102.3	555.2	103.8	25.2	1.000025
65000.0	60.4	-61.9		99.5	555.2	99.9	25.6	1.000022
65500.0	58.9	-61.5		97.3	555.3	97.7	25.2	1.000022
66000.0	57.2	-60.9		94.4	567.6	92.2	27.4	1.000021
66500.0	56.1	-60.1		91.3	558.6	81.4	27.5	1.000022
67000.0	54.9	-59.4		88.3	559.5	81.5	27.6	1.000020
67500.0	53.5	-58.7		86.9	573.5	85.8	25.8	1.000019
68000.0	52.2	-58.0		84.5	571.4	94.6	25.0	1.000017
68500.0	51.0	-57.3		82.3	572.4	99.7	25.8	1.000013
69000.0	49.8	-56.5		81.1	573.1	99.2	25.0	1.000015
69500.0	48.6	-57.0		78.3	572.7	98.7	25.3	1.000017
70000.0	47.4	-57.2		76.5	572.3	98.5	25.2	1.000017
70500.0	46.3	-57.6		74.9	571.9	98.3	25.0	1.000017
71000.0	45.2	-57.9		73.2	571.5	98.1	25.0	1.000015
71500.0	44.2	-57.9		71.5	571.0	98.0	25.9	1.000016
72000.0	43.1	-57.3		69.5	572.4	97.9	25.9	1.000015
72500.0	42.1	-56.7		67.3	573.2	101.5	25.7	1.000015
73000.0	41.1	-55.8		66.0	573.9	103.2	25.6	1.000015
73500.0	40.2	-55.3		64.3	574.7	106.5	25.0	1.000016
74000.0	39.2	-55.0		62.5	575.5	106.7	24.0	1.000016
74500.0	38.3	-54.4		61.0	575.2	105.3	23.3	1.000014
75000.0	37.4	-53.8		59.4	577.0	102.7	23.5	1.000013
75500.0	36.5	-53.2		57.9	577.7	99.5	23.7	1.000013
76000.0	35.7	-52.8		56.4	578.3	97.7	24.5	1.000013
76500.0	34.8	-52.9		55.1	578.2	99.8	25.4	1.000012
77000.0	34.0	-53.0		53.9	578.1	99.6	25.2	1.000012
77500.0	33.2	-53.1		52.5	578.9	97.9	25.3	1.000012
78000.0	32.5	-53.1		51.6	577.9	96.8	21.5	1.000011
78500.0	31.7	-53.2		50.2	577.3	95.9	20.8	1.000011
79000.0	31.0	-53.2		48.1	577.7	95.3	23.9	1.000011
79500.0	30.2	-53.4		46.0	577.5	96.8	23.9	1.000011
80000.0	29.6	-53.3		44.9	577.7	95.4	22.3	1.000013
80500.0	28.9	-53.1		43.7	577.9	93.9	23.8	1.000013
81000.0	28.2	-52.9		42.5	578.1	92.5	25.3	1.000013
81500.0	27.6	-52.8		41.5	578.4	88.6	25.6	1.000010
82000.0	26.9	-52.6		40.5	578.4	84.4	23.1	1.000009
82500.0	26.3	-52.4		41.5	578.2	91.8	29.7	1.000009
83000.0	25.7	-52.2		40.5	579.1	83.2	32.5	1.000009

ORIGINAL P...
OF POOR QUALITY

UPPER AIR DATA
100700Z
WHITE SANDS

STATION ALTITUDE 500.00 FEET MSL
6 JULY 84
ASCENSION NO. 550

GEODETIC COORDINATES
32.40043 LAT DEG
136.37333 LON DEG

GLOMERIC ALTITUDE MSL FEET	PRESSURE MILLIBARS	AIR TEMPERATURE DEGREES CELSIUS	REL. HUM. PERCENT	WIND DIRECTION DEGREES (TV)	WIND SPEED KNOTS	WIND DATA	INDEX OF REFRACTION
87500.0	15.1	-52.1	39.5	579.3	94.4	35.7	1.000019
87000.0	14.5	-51.9	39.5	579.5	95.4	37.9	1.000009
86500.0	14.0	-51.9	37.7	579.8	95.5	40.1	1.000005
86000.0	13.4	-50.9	36.7	580.7	87.5	42.2	1.000008
85500.0	12.9	-50.2	35.9	581.7	98.0	43.9	1.000005
85000.0	12.4	-49.5	34.9	582.6	97.4	44.7	1.000008
84500.0	11.9	-48.5	33.9	583.5	95.9	44.8	1.000005
84000.0	11.4	-48.1	33.1	584.4	95.5	45.4	1.000007
83500.0	10.9	-47.4	32.2	585.3	86.3	45.0	1.000007
83000.0	10.4	-46.7	31.4	585.2	96.1	46.7	1.000007
82500.0	9.9	-46.0	30.5	587.1	96.1	47.3	1.000007
82000.0	9.5	-45.6	29.3	587.7	95.2	47.9	1.000007
81500.0	9.1	-45.2	29.1	588.2	96.3	48.5	1.000005
81000.0	8.6	-44.8	28.4	589.7	96.1	49.3	1.000005
80500.0	8.2	-44.3	27.7	589.3	95.3	47.0	1.000005
80000.0	7.8	-43.9	27.1	589.8	94.5	45.7	1.000006
79500.0	7.4	-43.5	26.4	590.4	84.2	44.9	1.000005
79000.0	7.0	-43.1	25.8	590.9	94.5	45.3	1.000005
78500.0	6.6	-42.7	25.2	591.5	94.9	45.6	1.000005
78000.0	6.2	-42.4	24.5	591.7	95.5	45.0	1.000005
77500.0	5.9	-42.2	24.0	592.0	97.7	45.6	1.000005
77000.0	5.6	-42.1	23.5	592.2	89.9	45.8	1.000005
76500.0	5.2	-41.9	22.9	592.5	91.9	47.4	1.000005
76000.0	4.9	-41.7	22.4	592.7	93.7	45.7	1.000005
75500.0	4.6	-41.5	21.9	593.0	94.5	45.8	1.000005
75000.0	4.3	-41.5	21.6	593.2	96.0	46.9	1.000005
74500.0	4.1	-41.1	20.9	593.5			1.000005
74000.0	3.9	-40.9	20.4	593.7			1.000005
73500.0	3.6	-40.7	20.0	593.9			1.000004
73000.0	3.3	-40.5	19.5	594.2			1.000004
72500.0	3.1	-40.2	19.1	594.4			1.000004
72000.0	2.9	-40.1	18.4	594.7			1.000004

STATION ALTITUDE 1979.03 FEET MSL
 8 JULY 64
 ASCENSION NO. 580

PRV SIGNIFICANT LEVEL DATA
 1000 FT
 WHITE SANDS

GEODETIC COORDINATES
 32.45363 LAT DEG
 106.37053 LON DEG

GEOPENTRAL ALTITUDE DECA METERS	DIRECTION DEG (TR)	WIND DATA		E-W MPS	DEL PT DF DEG C	TEMPERATURE		PRESSURE MILLIBARS
		SPED MPS	V-S MPS			AIR DEG C		
1035.	9799.00	9799.00	-9999.00	-9799.00	99	-60.1	1.240+1	
1507.	85.	0.	-2.	-21.	99	-42.5	1.650+1	
2462.	86.	4.	-2.	-24.	99	-45.1	2.000+1	
2563.	96.	1.	-1.	-23.	99	-51.7	2.400+1	
419.	96.	11.	1.	-11.	99	-53.4	3.000+1	
1303.	100.	13.	2.	-12.	99	-52.8	3.500+1	
1354.	98.	17.	2.	-13.	99	-53.1	4.450+1	
1592.	96.	13.	2.	-12.	99	-56.7	5.000+1	
1995.	87.	14.	-1.	-14.	99	-51.3	5.360+1	
1853.	94.	17.	1.	-13.	99	-64.7	7.000+1	
1753.	115.	6.	3.	-5.	99	-58.6	8.520+1	
1567.	117.	7.	3.	-7.	99	-71.2	1.000+2	

** WIND DATA NOT COMPUTED DUE TO MISSING RAW AZIMUTH AND ELEVATION ANGLES.

Chart
 Dr. [unclear]

STATION ALTITUDE 5925.0 FEET 'SL
 8 JULY 54
 ASCENSION NO. 356

MANDATORY LEVELS
 1°00'22"166
 WHITE SANDS

GEODETTIC COORDINATES
 32.43043 LAT DEG
 106.37733 LON DEG

ORIGINAL PAGE IS
 OF POOR QUALITY

PRESSURE MILLIBARS	GEOG. ALTITUDE FEET	TEMPERATURE		REL. HUM. PERCENT	WIND DATA	
		AIR DEGREES CENTIGRADE	DWPOINT CENTIGRADE		DIRECTION DEGREES(TV)	SPEED KNOTS
800.0	5715.	22.7	9.1	62.	190.9	7.1
800.0	6740.	20.2	7.6	46.	193.9	10.8
750.0	3555.	15.1	5.3	49.	205.4	7.0
700.0	10467.	11.5	2.5	56.	126.9	6.5
650.0	12651.	6.1	-0.5	53.	34.1	12.3
600.0	14517.	2.5	-14.7	27.	101.1	13.4
550.0	16911.	-0.8	-21.5	19.	137.4	15.7
500.0	19389.	-7.1	-26.7	17.	143.7	14.6
450.0	22065.	-10.5	-30.0	18.	152.7	19.8
400.0	25207.	-17.0	-36.1	21.	150.4	15.3
350.0	28243.	-23.5	-40.9	20.	147.8	10.2
300.0	31875.	-33.1	-48.0	21.	92.5	4.5
250.0	35990.	-42.9			22.5	9.1
200.0	40511.	-53.7			358.6	17.7
175.0	43532.	-59.5			341.2	8.6
150.0	46717.	-66.0			27.3	14.9
125.0	50338.	-69.2			97.3	5.3
100.0	54577.	-71.2			117.1	14.4
80.0	59159.	-64.1			65.1	7.3
70.0	61784.	-66.7			31.3	25.0
50.0	64997.	-61.8			94.1	25.5
50.0	68642.	-56.7			90.4	26.0
40.0	72275.	-55.4			105.5	24.9
30.0	79343.	-53.6			96.5	21.2
25.0	83211.	-52.0			84.5	35.5
20.0	86063.	-45.1			85.7	47.3
15.0	94355.	-41.7			92.7	67.1

** AT LEAST ONE ASSUMED RELATIVE HUMIDITY VALUE WAS USED IN THE INTERPOLATION.

OF POOR QUALITY

SECTETIC COORDINATES
 32.4J043 LAT DEG
 106.37033 LON DEG

MRN MANDATORY LEVELS
 1000000166
 WHITE SANDS

STATION ALTITUDE 229.0 FEET ASL
 8 JULY 84
 0300 HRS MST
 ASCENSION NO. 255

GEOPOTENTIAL ALTITUDE DECAHETERS	COLLECTION DEG (TN)	WIND DATA		DEW PT DEF DEG C	TEMPERATURE		PRESSURE MILLIBARS
		SPEED MPS	V-S MPS		AIR DEG C		
2875.	97.	26.	1.	99	-41.7	1.500+1	
2652.	66.	24.	-2.	99	-44.1	2.000+1	
2536.	64.	14.	-2.	99	-52.0	2.500+1	
2419.	97.	11.	1.	99	-53.4	3.000+1	
2233.	107.	14.	4.	99	-55.4	5.000+1	
2122.	96.	12.	2.	99	-56.7	5.000+1	
1973.	98.	14.	2.	99	-61.8	6.000+1	
1883.	94.	17.	1.	99	-54.7	7.000+1	
1802.	86.	4.	-0.	99	-64.1	3.000+1	
1667.	117.	2.	3.	99	-71.2	1.000+2	
1524.	91.	3.	0.	99	-69.2	1.250+2	
1424.	27.	9.	-7.	99	-56.0	1.500+2	
1329.	341.	6.	-4.	99	-50.5	1.750+2	
1244.	358.	9.	-9.	99	-51.9	2.000+2	
1097.	27.	5.	-4.	99	-42.9	2.500+2	
972.	97.	2.	0.	15	-33.3	3.000+2	
831.	148.	5.	4.	17	-23.5	3.500+2	
762.	150.	5.	2.	17	-17.0	4.000+2	
673.	107.	10.	10.	19	-10.5	4.500+2	
571.	144.	7.	6.	20	-7.1	5.000+2	
515.	137.	2.	6.	21	-8	5.500+2	
466.	101.	2.	1.	17	2.5	5.000+2	
350.	84.	3.	-1.	27	5.1	5.500+2	
319.	125.	2.	1.	99	11.5	7.000+2	
251.	204.	4.	7.	11	15.1	7.500+2	
205.	194.	6.	5.	13	20.2	3.000+2	
152.	191.	6.	4.	14	22.7	3.500+2	